Journal of Applied Polymer Science

Polypropylene Fibers Fabricated via a Needleless Melt-Electrospinning Device for Marine Oil-Spill Cleanup

Haoyi Li,[1,2] Weifeng Wu,[1] Mahmoud M. Bubakir,[1] Hongbo Chen,[1] Xiangfeng Zhong,[1] Zhaoxiang Liu,[1] Yumei Ding,[1] Weimin Yang[1,2]

[1]College of Mechanical and Electrical Engineering, Beijing University of Chemical Technology, Beijing 100029, China
[2]State Key Laboratory of Organic–Inorganic Composites, Beijing University of Chemical Technology, Beijing 100029, China
Correspondence to: W. Yang (E-mail: yangwm@mail.buct.edu.cn)

ABSTRACT: Ultrafine polypropylene (PP) fibers as oil sorbents were fabricated via a needleless melt-electrospinning device and were characterized by scanning electron microscopy and contact-angle analysis. PP fibers of various diameters and porosities were obtained by the manipulation of the applied electrical field. The effects of the fiber diameter and porosity on the oil-sorption capacity and oil-retention behavior were investigated. The experimental results demonstrate that for fiber diameter on the microscale, the porosity played a paramount role in determining the oil-sorption capacities. The maximum oil-sorption capacity of the resulting PP fibers with regard to motor oil and peanut oil were 129 and 80 g/g, respectively; these values were approximately six to seven times that of commercial PP nonwoven fabricated through the melt-blown method. In addition, even after seven sorption/desorption cycles, the oil-sorption capacity of the chosen sample was still maintained around 80 g/g, and above 97%, oil could be recovered. This indicated excellent reusability and recoverability. © 2013 Wiley Periodicals, Inc. J. Appl. Polym. Sci. **2014**, *131*, 40080.

KEYWORDS: applications; electrospinning; fibers

Received 29 August 2013; accepted 19 October 2013
DOI: 10.1002/app.40080

INTRODUCTION

Currently, there is an increasing demand for oil and its derivatives in the automobile industry and in chemical engineering. When oil is exploited, transported, stored, and used, the risk of oil spills exist; this can not only lead to energy loss but can also cause catastrophic damage to the ecological environment.[1,2] The BP Deepwater Horizon oil spill in the Gulf of Mexico, the largest marine oil spill in history, caused extensive damage to marine and wildlife habitats and the fishing and tourism industries, as well as to human health. Remediations in response to oil spills in seawater generally comprise physical methods (e.g., sorbents, booms, skimmers), chemical methods (e.g., *in situ* burning, dispersion), and bioremediation, among which physical recovery by the concentration and transformation of oil from the liquid phase to the semisolid or solid phase with oil sorbents is considered to be one of the most efficient and cost-effective countermeasures.[3–5] Hydrophobicity and oleophilicity are the most essential features of sorbents for oil–water separation. Other properties of ideal oil sorbents include a high oil-sorption capacity, high oil retention over time, good buoyancy, recoverability of absorbed oil, reusability, and biodegradability. Oil sorbents generally can be classified into three types, namely inorganic mineral materials (e.g., perlite, vermiculite, diatomite), natural organic materials (e.g., corn straw, milkweed, cotton, kapok), and synthetic organic materials [e.g., polypropylene (PP), polyurethane foam]. Among them, synthetic organic material PP in particular has been widely used.[6–11] PP is inherently a hydrophobic–oleophilic material with a low density and large-scale fabrication; this renders it particularly suitable for marine oil-spill cleanup.[12] Traditional PP nonwovens fabricated by a melt-blown method, however, suffer a relatively low oil-sorption capacity (ca. 20 g/g) compared with other materials because of its large fiber diameter (15–20 μm) and low porosity.

Electrospinning, a straightforward and versatile technique for generating fibers on the microscale and nanoscale with an attenuating polymer solution or melt through a nozzle under an electrostatic force has gained increasing attention from researchers worldwide.[13–15] It can be categorized into solution electrospinning (SES) and melt electrospinning (MES). SES has already been applied recently in the fabrication of oil sorbents. In 2011, Zhu et al.[16] first reported the feasibility of solution-electrospun poly(vinyl chloride)/polystyrene fibers for oil-spill cleanup, and its oil-sorption capacities for motor oil, peanut oil, ethylene glycol, and diesel were 146, 119, 81, and 38 g/g, respectively. These values were five to nine times higher than

that of a commercial PP nonwoven. Wu et al.[17] investigated the effects of the fiber diameter and surface morphology on the oil-sorption performance of electrospun polystyrene fibers and found that thinner and porous structured fibers possessed a higher sorption capacity. Afterward, a series of studies were conducted by Lin and coworkers,[18,19] who obtained electrospun fibers with hierarchical structures by tuning the parameters, including the relative humidity, molecular weight, solvent composition, and solution concentration. To promote their reusability, he further improved the mechanical properties of the resulting fibers via multinozzle electrospinning and coaxial electrospinning.[20,21]

All of the abovementioned fabricating methods of oil sorbents are SES, but to the best of our knowledge, no work has been done to fabricate ultrafine PP fibers for oil–water application via MES because the high viscosity and low conductivity of the molten polymer prevent it from generating ultrafine fibers.[22] In addition to the intrinsic problems of the materials, MES needs to be operated at an elevated temperature and a higher voltage; this makes MES devices much more complicated than SES devices. Nevertheless, MES still shows an edge over SES in the electrospinning of thermoplastic polymers such as PP; this makes it difficult to find a suitable solvent at ambient temperature. In this study, a needleless MES device designed and specifically tailored for industrialization with a high throughput was used. PP fibers with different fiber diameters and porosities were obtained through the variation of the electric field to study the effect of the fiber diameter and porosities on the oil-sorption capacity and oil-retention performance. Furthermore, the oil/water selectivity, reusability, and recoverability of the resulting fibers were investigated.

EXPERIMENTAL

Materials

Polypropylene (PP6820) with a melt flow rate of 2000 g/10 min (tested at 230°C) was procured from Shanghai Expert in the Developing of New Material Co. and was used as received. In our previous studies, the melt flow rate, a direct reflection of the viscosity, was found to be the most important parameter governing the fiber diameter,[23] so PP with a melt flow rate as high as 2000 g/10 min was used as a raw material to generate ultrafine fibers. Two typical oils, motor oil and peanut oil, were chosen in this study, and their physical properties are listed in Table I.

Table I. Physical Properties of Motor Oil and Peanut Oil

	Viscosity at 25°C (mPa s)	Density at 25°C (g/cm^3)
Motor oil	220	0.801
Peanut oil	41	0.863

Electrospinning

Figure 1 shows a self-designed MES device, which was composed of six major components: a high-voltage power supply, a heating system, an air pressure gun, a copper circular ring serving as electrode A, a needleless cone-shaped nozzle, and a collecting device. The high-voltage supply device, purchased from Tianjin High Voltage Power Supply Plant (China), provided a maximum output of 100 kV and a maximum current output of 2 mA. The electric heating ring with a power of 300 W was custom built. Three features of our device must be highlighted:

1. The needleless nozzle could generate multiple Taylor cones around the bottom edge of the nozzle; hence, a high throughput could be achieved.
2. The air current provided by an air pressure gun further strengthened the stretching force acting on the jets. More importantly, it could contract the flying jets with the pressure difference between the air current and the atmosphere to prevent the polymer jets from being attracted by the inner circle of electrode A.

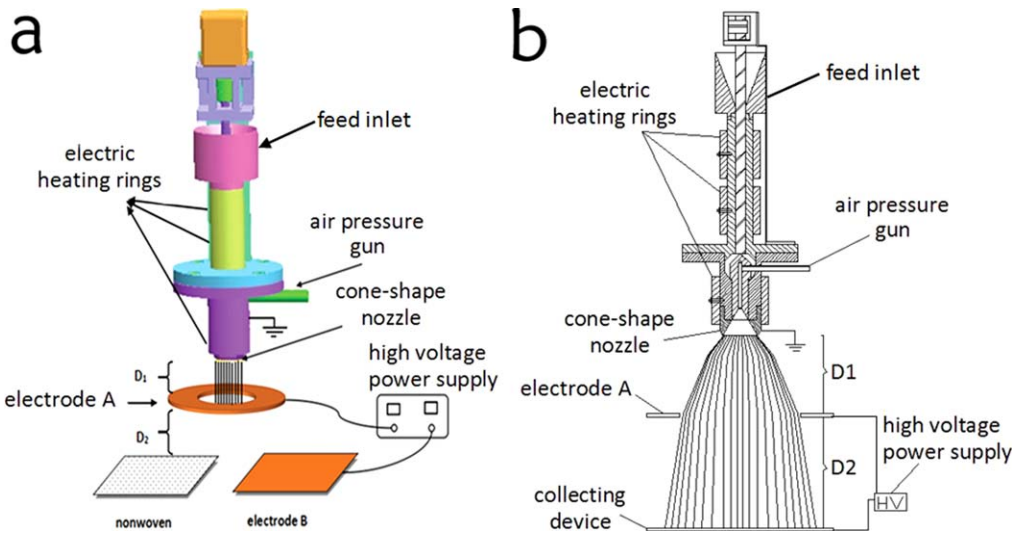

Figure 1. Three-dimensional and two-dimensional schematics of a self-designed needleless MES device. [Color figure can be viewed in the online issue, which is available at wileyonlinelibrary.com.]

3. Two kinds of collecting devices were applied, namely, the nonwoven and electrode B. The nozzle was grounded to prevent interference between the high-voltage supply and temperature sensors.

The electrospinning process was carried out in a humidity of 25% at 24°C. Temperatures for three heating rings were set to 180, 200, and 230°C, respectively. The distances between the nozzle and electrode A (marked as D_1 in Figure 1) and the distance between electrode A and the collecting device (marked as D_2 in Figure 2) were set to 45 and 130 mm, respectively. We controlled the melt feeding rate at approximately 9.82 g/h by setting the revolving speed of the lead screw at 20 rpm. Four different voltages (27, 30, 33, and 36 kV) were applied to electrode A. First, a nonwoven fibrous mat was used as the collecting device, and fiber samples S1, S2, S3, and S4 were collected. Then, electrode B, with a voltage of 65 kV, was used as the collecting device, and fiber samples D1, D2, D3, and D4 were collected.

Characterization

The fiber diameter and surface morphology of the electrospun PP fibers were examined by scanning electron microscopy (SEM; S-4700, Hitachi, Ltd., Japan). Before observation, all of the fibers were platinum-coated. Image processing software (Image J 2X) was applied to calculate the average fiber diameters and standard deviations from 100 measurements of each sample at each spinning voltage.

Interaction between water or oil and the resulting fibers was quantified by a contact-angle system (Dataphysics, Germany) at 25°C. Two microliters of deionized water were dropped on the surfaces of 0.1 g of S2 and D3. Images of the solid/liquid interface were captured by a charge-coupled device camera. The average contact-angle value was obtained by measurement of the same sample at five different positions.

Test of the Oil-Sorption Capacity and Oil-Retention Performance

To study the maximum oil-sorption capacity of the as-spun PP fibers, a sorption test was conducted by the placement of 0.1 g of sorbent into a 500-mL beaker containing 150 mL of oil. After about 60 min of sorption, the oil-saturated sorbent was removed with a nipper and placed onto a digital balance, whereupon the sorbed oil started to drip from the sorbent. The mass of the sorbent was recorded after 0, 5, 10, 15, 20, 25, and 30 min, respectively. Finally, an oil-retention curve of each sample could be obtained. All of the oil-sorption tests were conducted at 25°C. The oil-sorption capacities of all of the sorbents was determined by the following equation:

$$Q=\frac{m_t-(m_i+m_w)}{m_i}\times 100\% \quad (1)$$

where Q is the oil-sorption capacity (g/g); m_i is the initial weight of the dry sorbent, which was set as 0.1 g; m_t is the total weight of the oil-saturated sample after 5 min of oil drainage (g); and m_w is the weight of the adsorbed water (g). All experiments were repeated independently five times, and the standard deviations were calculated. To study the selective sorption of oil from water, a 500-mL beaker containing 300 mL of water and 150 mL of motor oil was used. After 60 min of sorption, the oil sorbent was put into an oven at a temperature of 100°C for 5 min; then, the mass of the sorbent was recorded, and the oil-sorption capacity was calculated by the means mentioned previously.

Test of Porosity[16]

A columned box with a diameter of 5 cm and a height of 5 cm was used to calculate the porosity of the resulting PP fibers. By filling the columned box with a fibrous mat, we calculated the total volume and weight of the fibrous mat. Provided the density of PP (0.91 g/cm^3) was unchanged before and after MES, we could estimate the porosity through the weight of the fibrous mat divided by the product of the density of PP and the total volume of the fibrous mat.

Test of the Reusability and Recoverability

After the initial sorption test, the oil was removed from the oil-loaded sorbents (S4 and D4 were chosen for the test) with a vacuum pump. Then, the samples were weighed and subject to the next sorption test. The sorption/desorption process was repeated for seven cycles to evaluate the reusability and recoverability of the resulting PP fibers.

RESULTS AND DISCUSSION

Morphology Analysis

Melt-electrospun PP fibers were collected with two kinds of collecting devices: a commercial PP nonwoven and electrode B, applied with a constant voltage of 65 kV. With the absence of electrode B, the electric field only existed between the nozzle and electrode A, and the electric field intensity was Voltage A/D1. With the presence of electrode B, there were two major kinds of electric fields, which existed between the nozzle and electrode A and between the electrodes A and B, respectively. Their intensity could be calculated by Voltage A/D1 and (Voltage B − Voltage A)/D2, respectively. In addition, the coupling between these two electric fields also contributed to the enhancement of the overall electric field intensity in this system. As the electrostatic force was the major driving force and played an imperative role in determining the diameter of the resulting fibers during electrospinning, the voltage applied to electrode A was varied from 27 to 36 kV to manipulate the diameter and morphology of the as-spun fibers. With the increased voltage from 27 to 36 kV, the electric field intensity between the nozzle and electrode A linearly increased from 27 kV/45 mm to 36 kV/45 mm, whereas a decrease in the electrical field intensity between electrode A and B from 38 kV/130 mm to 29 kV/130 mm could be expected.

Figure 2 demonstrates the optical photos of the as-spun PP fibers. As shown in Figure 2(a), the sample S2 exhibited a fluffy, cottonlike appearance, whereas sample D2 exhibited a compact, clothlike appearance. The experimental results of the porosities are listed in Table II. As shown, there was little difference among fibers generated in the same electric field system but a relatively wide variance between the different electric field systems. The PP fibers of D1–D4 possessed lower porosities than the PP fibers of S1–S4; this was in agreement with their optical photos. This could be ascribed to the much stronger adhesion between the fibrous films of each layer under the attraction of electrode B, which decreased the space of interfiber voids and, thus, the porosity.

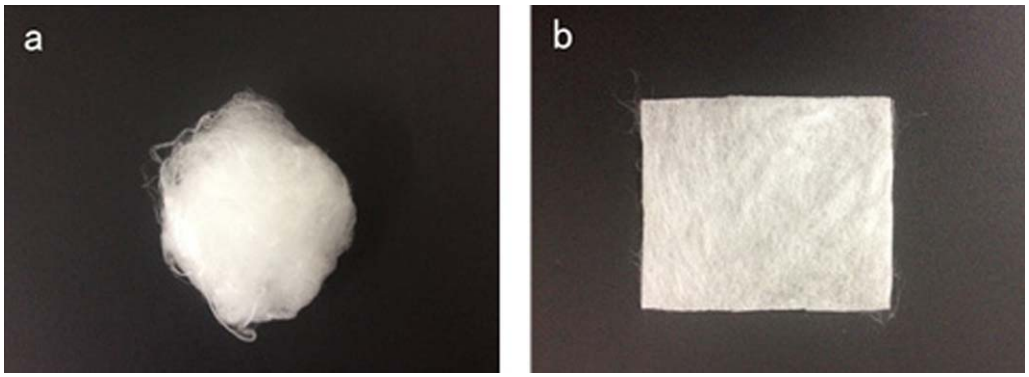

Figure 2. Optical photos of (a) sample S2 collected with the nonwoven and (b) sample D2 collected with electrode B. [Color figure can be viewed in the online issue, which is available at wileyonlinelibrary.com.]

SEM images of the PP fibers generated via MES under different voltages are shown in Figure 3. As shown, the resulting electrospun fibers randomly oriented with a smooth surface and threadlike structure in contrast to the porous structured fibers fabricated in SES. The smooth exterior and solid interior morphologies of the melt-electrospun fiber guaranteed its superior mechanical performance over those generated from SES; this favored its reusability. There were also large amounts of interfiber voids in the range 10–90 μm; this provided sufficient storage space for the absorbed oil. The void sizes were obtained roughly by measurement of the distance of two adjacent fibers with the image processing software Image J in the SEM images.

As is shown in Figure 4, the diameter of the PP fibers fabricated with a single electrode experienced a marked decrease from 7.14 to 3.35 μm when the applied voltage was increased from 27 to 30 kV; this was followed by an increase from 3.35 to 4.24 μm when the applied voltage was increased from 30 to 36 kV. The diameter of the PP fibers collected by electrode B showed a similar trend, with the minimum fiber diameter being 1.89 μm at a voltage of 33 kV. The second electrical field between electrodes A and B provided an additional stretching force so finer fibers were formed as expected. It is commonly acknowledged that to some extent, the fiber diameter is inversely proportional to the applied voltage, but in our study, the fiber diameter increased when the applied voltage to electrode A was increased beyond 30 or 33 kV. Another interesting phenomenon was that when electrode A was applied with lower voltages, the PP fibers generated by a single electrode tended to be smaller in diameter than those formed by double electrodes. One possible explanation for these phenomena was that when the electrical field intensity became too high, Taylor cones tended to be larger; thus, more molten polymer would be pulled out by the stronger electric force, and coarser PP fibers were consequently obtained. Another reason was that the stronger stretching force created by the stronger electrical field intensity accelerated the collecting process so that the fluid jets failed to undergo sufficient attenuation. Subsequent work based on electric field analysis will reveal the underlying mechanism of the fiber-formation process. Overall, the PP fibers produced through MES exhibited a smaller fiber diameter and higher porosity than the commercial PP nonwoven; this may have contributed to the adsorption and adhesion of oil onto the fiber surfaces and into the interconnected voids among the fibers.

Contact-Angle Analysis

The morphologies of the fibrous mat and the liquid drop on their surfaces are shown in Figure 5. All of the as-spun PP fibers exhibited a higher hydrophobicity than the commercial PP nonwoven with a thick fiber diameter (ca. 15–20 μm) formed via melt blowing.

Superhydrophobic surfaces with a water contact angle larger than 150° have attracted extensive interest in academia because of their versatile applications. A superhydrophobic surface can be obtained by the introduction of a hierarchical micrometer-scale roughness on the surface with a low surface energy according to the theory of the roughness-induced hydrophobicity proposed by Cassie et al.[24,25] Cho et al.[26] obtained electrospun PP fibers with diameters ranging from 0.8 to 9.6 μm from the solution and melt. It has been observed that there is only a slight variance of wettability among fibers of different diameters; this suggests that fiber diameters under 10 μm are sufficient to offer a surface roughness to achieve the superhydrophobicity of a PP fibrous mat via electrospinning. However, Figure 5 shows that the fiber samples S2 and D3 exhibited a water contact angle of 135 and 130°; these values were well below 150°but still confirmed its hydrophobic nature. In contrast, when samples S2 and D3 were tested with motor oil, the oil droplets immediately spread on the surface of fibrous mat with an oil contact angle of 0° less than 1 s; this indicated its superoleophilic properties and high rate of oil uptake. Therefore, the MES of PP, which is inherently hydrophobic and superoleophilic, can offer a more straightforward and one-step approach to produce superhydrophobic fibrous films in contrast to other methods, which involve either the complicated synthesis of hydrophobic and hydrophilic materials or additional coating.[27,28]

Oil-Sorption Capacity and Oil-Retention Behavior

To determine the maximum oil-sorption capacity of the resulting PP fibers, the sorption test was first performed in a pure oil medium without any water. Experimental curves demonstrated that the retention behavior of the all as-spun fibers followed almost the same trend. As shown in Figure 6, the oil-retention ratio of a normal sorbent usually undergoes three distinct

Table II. Major Parameters for the Resulting Fibers and Oil-Sorption Tests

Sample	Sample properties			Motor oil				Peanut oil			
	Fiber diameter (μm)	Porosity (%)	Theoretical SSA (m^2/g)	Initial sorption capacity (g/g)	Oil reduction rate 1 (%)	Sorption capacity (g/g)	Oil reduction rate 2 (%)	Equilibrium state (g/g)	Initial sorption capacity (g/g)	Oil reduction rate 1 (%)	Sorption capacity (g/g)	Oil reduction rate 2 (%)	Equilibrium state (g/g)
S1	7.14	97.5	0.62	165	47	88	76	40	108	53	51	71	31
S2	3.35	98.6	1.31	221	42	129	71	64	150	47	80	65	52
S3	3.99	98.4	1.10	194	41	115	70	58	138	51	67	68	44
S4	4.24	98.4	1.04	197	49	101	72	56	147	57	63	70	44
D1	7.32	93.8	0.60	96	30	67	57	41	62	47	33	47	33
D2	3.67	93.8	1.20	121	31	83	58	51	86	22	67	44	48
D3	1.89	94.3	2.33	157	27	114	59	65	102	23	79	44	57
D4	2.37	94.8	1.85	163	36	105	64	59	91	24	69	36	58

Oil reduction rates 1 and 2 refer to the oil reduction rates during the first 5 min and the first 30 min, respectively.

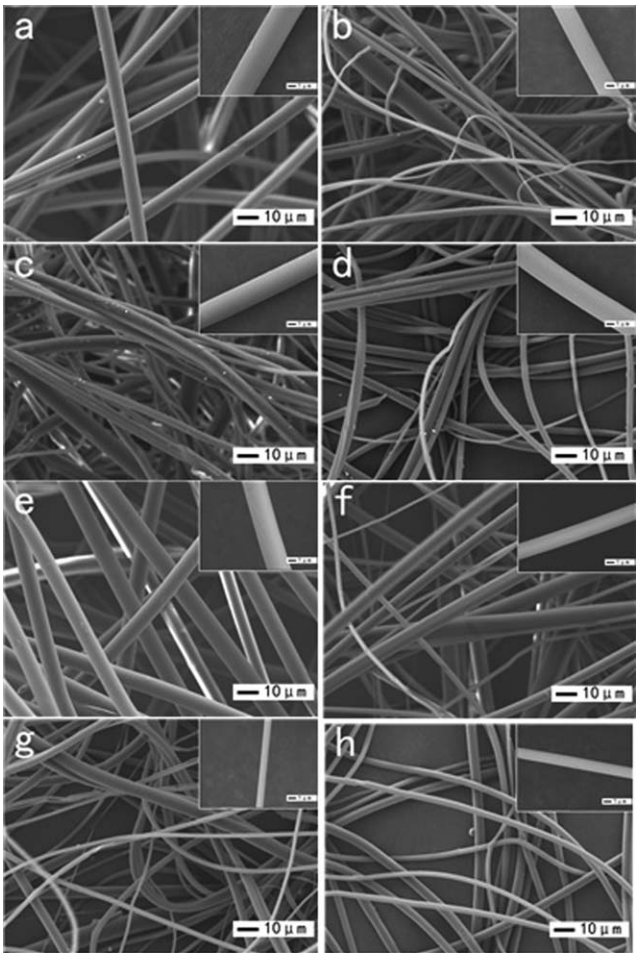

Figure 3. SEM images of PP fibers generated at voltages of 27, 30, 33, and 36 kV and collected with (a–d) the nonwoven or (e–h) electrode B.

periods after it is removed from the oil medium. During the first 5 min, the oil loosely adsorbed dripped from the oil sorbent sharply so there was a dramatic reduction in the oil-

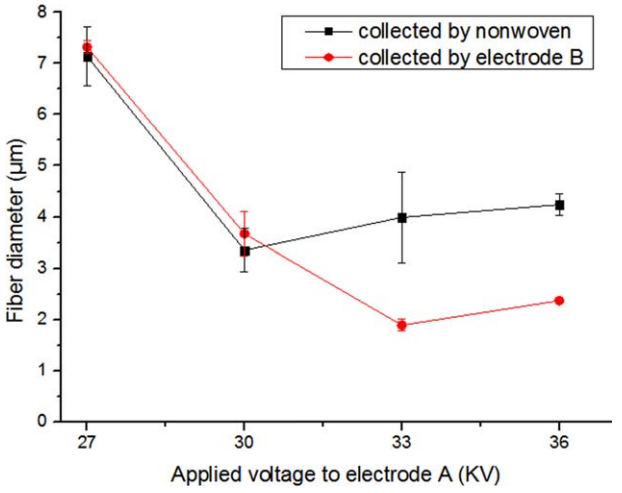

Figure 4. Curves of average diameters of the resulting fibers collected with the nonwoven and electrode B. [Color figure can be viewed in the online issue, which is available at wileyonlinelibrary.com.]

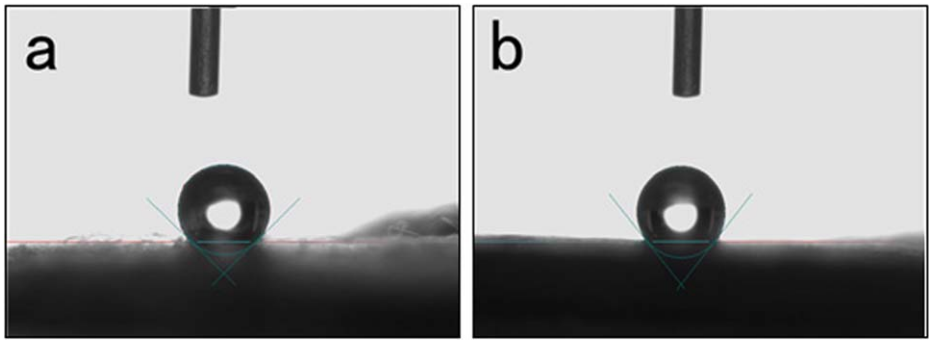

Figure 5. Contact-angle analysis of (a) S2 and (b) D3. [Color figure can be viewed in the online issue, which is available at wileyonlinelibrary.com.]

retention curve. Then, the release rate of oil slowed down substantially from 5 to 15 or 20 min; this is called the second period or transition period. Subsequently, a leveling out was seen in the third period; this indicated the ceasing of oil release from the sorbent.[29] There were also three distinct points in the retention curve at 0 s, 5 min, and around 15–20 min; these represent the initial sorption capacity, oil-sorption capacity, and equilibrium state, respectively.

As shown in Figure 6(a), there was a great difference between the oil-sorption capacity of the as-spun fibers with different diameters and the similar porosity. The sorption capacity diminished along with the increase in fiber diameter in the same porosity range. For instance, for PP fibers with higher porosities, S2 with the minimum diameter of 3.35 μm possessed the highest sorption capacity of 129 g/g for motor oil, followed by S3 (3.99 μm), S4 (4.24 μm), and S1 (7.14 μm) with a sorption capacity of 115, 101, and 88 g/g, respectively. The increased sorption capacity was attributed to the increased specific surface area (SSA), which offered a large amount of area for the adsorption of oil. Lin et al.[19] obtained the theoretical SSA of

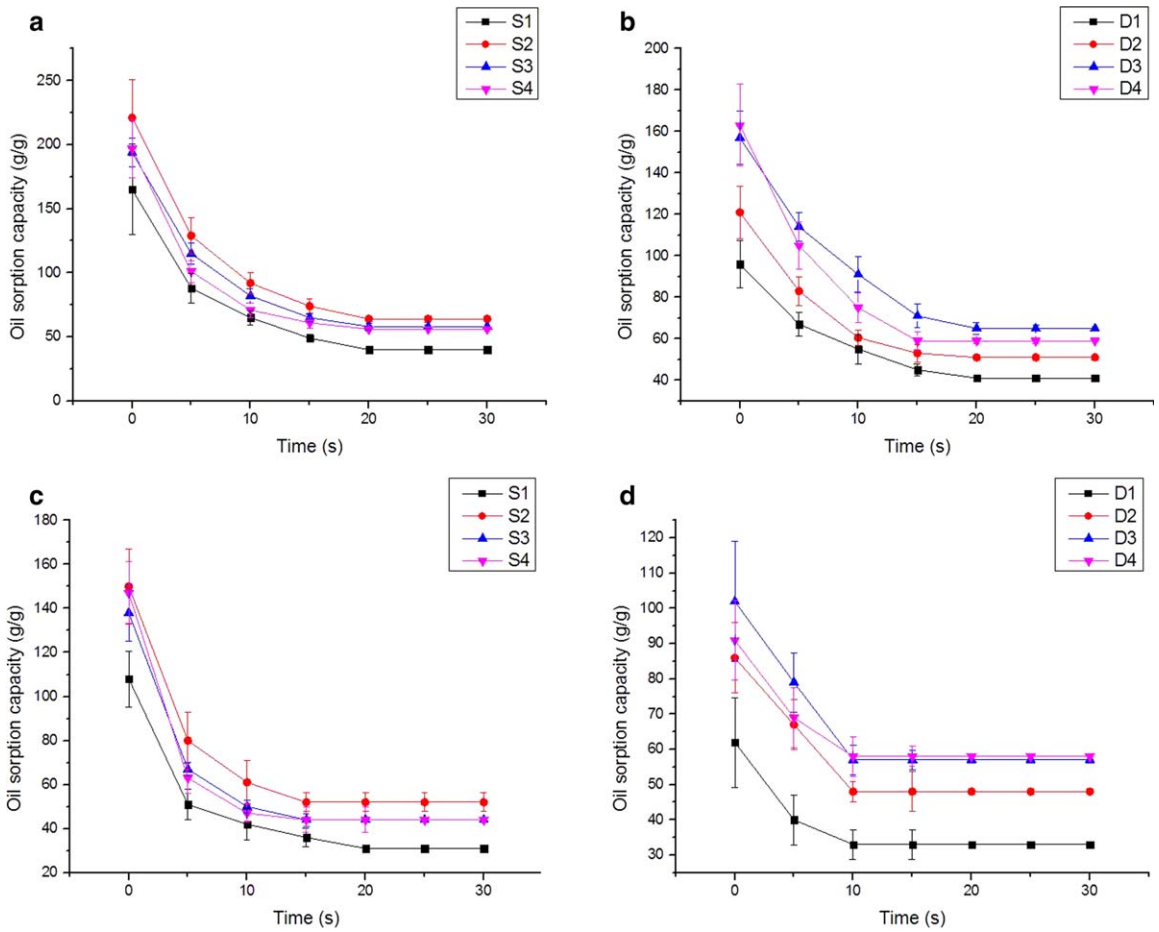

Figure 6. Oil desorption kinetics curves of the PP fibers for (a,b) motor oil and (c,d) peanut oil. [Color figure can be viewed in the online issue, which is available at wileyonlinelibrary.com.]

the solid fiber with a circular cross section by employing mathematical calculation if the length of every single fiber is infinite. The SSA of the resulting fibers per gram is given in eq. (2):

$$S_t = \frac{4}{\rho D} \quad (2)$$

where S_t is the theoretical SSA of the resulting fibers (m^2/g), ρ is the density of the PP fibers provided that the density of PP before and after MES is unchanged ($\rho = 0.91$ g/cm^3), and D is the average diameter of the PP fibers (μm).

Equation (2) indicates that the S_t of resulting fibers was inversely proportional to their average diameter when their density was a fixed value. Therefore, to achieve a higher oil-sorption capacity, the production of a sorbent with a thinner fiber diameter was necessary. Figure 7 shows the relationship between the PP fiber diameter and the theoretical SSA. For fibers larger than 1 μm, with increasing fiber diameter, the theoretical SSA became increasingly insensitive to the fiber diameter. This was why there was not much obvious correlation between the fiber diameter and sorption capacity in the first few times of our oil-sorption test. Only after a constant repetition of experiments, regular results were obtained.

The comparison between Figure 6(a,b) suggests that fibers S1–S4, collected by the nonwoven, exhibited a higher initial sorption capacity than those (D1–D4) collected by electrode B. S2 presented a higher initial sorption capacity of 221 g/g compared with D3, which presented an initial sorption capacity of just 157 g/g. This meant that fibers with a higher porosity possessed a higher initial sorption capacity. However, S4 released 49% of its sorbed oil in the first 5 min, and the oil released from S1, S2, and S4 were well above 40%. In the case of samples D1–D4, the oil release rates were all around 30%, with the minimum rate being 27%. Nonetheless, the oil-sorption capacities of S1–S4 were still slightly higher than those of D1–D4 even after a release of oil in great quantity. For example, S3, with a fiber diameter of 3.99 μm and a porosity of 98.4%, exhibited a sorption capacity of 115 g/g; this was slightly higher than that of D3, with a fiber diameter of 1.89 μm and a porosity of 94.3%. Therefore, we concluded that a high porosity played a paramount role in determining the high capacity of the oil sorbents; this was also in agreement with the results of previous studies.[30] In other words, the significance of the fiber diameter was larger than that of the fiber fineness for the oil-sorption capacity of microscale fibers. The high porosity was attributed to the tremendous numbers of voids among the fibers; thus, it provided large amounts of storage space as an oil vessel for adsorbed oils. During the extraction and transformation of oil from a liquid to semisolid or solid phase with an oil sorbent in a marine oil spill, one should bear in mind that an oil-saturated sorbent needs to be removed from sea surface without significant oil drainage in a certain amount of time. As a result, the oil-retention performance is also a crucial factor of an ideal sorbent. In this study, fiber samples S1–S4 released over 70% of the adsorbed motor oil after 30 min of drainage. Therefore, a further enhancement in the oil-retention capacity was necessary.

The physical properties of oil, such as density, surface tension, and viscosity, could also influence the sorption capacity and the retention behavior as well. Previous studies have demonstrated that the sorption capacity of a certain sorbent with regard to different kinds of oils exhibit an inconspicuous relation to their density and surface tension but an increasing tendency along with increasing viscosity.[16–21] As illustrated in Table II, the sorption performance of peanut oil with a lower viscosity was lower than that of motor oil with a higher viscosity.

The oil-sorption capacity of the as-spun PP fibers in the motor oil–water bath was tested. It was observed that the PP fibers showed a great affinity to oil and a repellency to water. All of the tested fibers were entirely immersed in motor oil within just 5 s. Figure 8 shows that the oil-sorption capacity of the resulting fibers in pure motor oil and the oil–water bath were almost the same. Because of experimental errors, there was literally no difference in the sorption performance in the pure oil system or the oil–water system; this confirmed its feasibility for oil-spill recovery at sea. During the process of oil sorption, we also

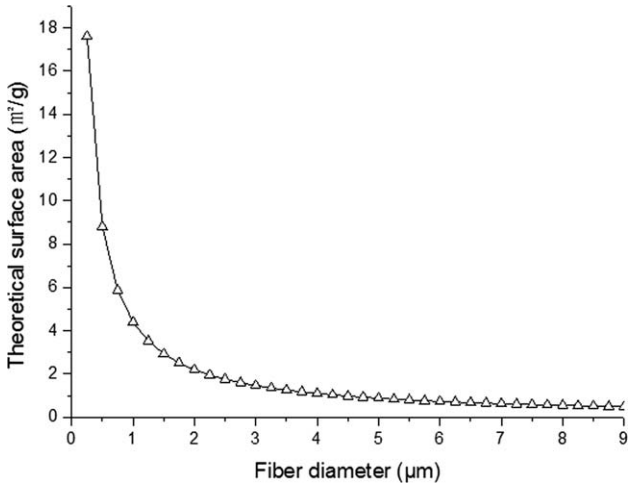

Figure 7. Diameter of the melt-electrospun PP fiber versus the theoretical SSA.

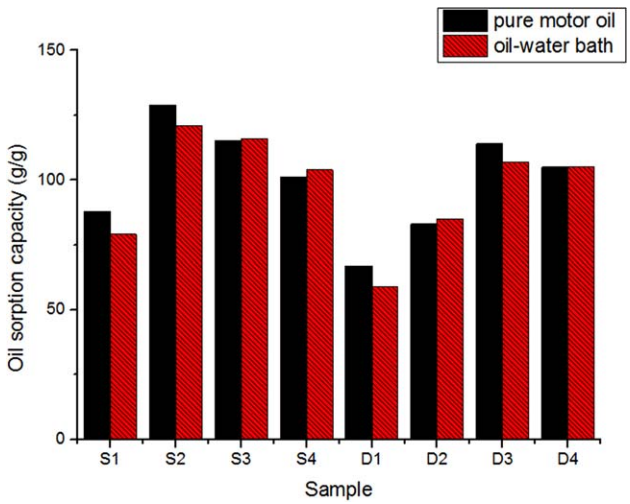

Figure 8. Comparison of the oil-sorption capacities of the sorbents in pure motor oil and oil–water baths. [Color figure can be viewed in the online issue, which is available at wileyonlinelibrary.com.]

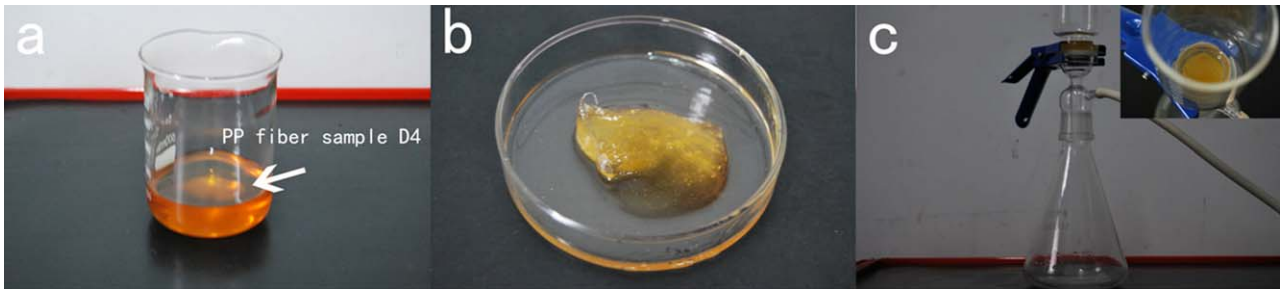

Figure 9. Operation process of oil sorption and desorption. [Color figure can be viewed in the online issue, which is available at wileyonlinelibrary.com.]

observed that all of the as-spun PP fibers with a low density exhibited a high buoyancy; this kept the sorbent floating over the oil–water bath while completely repelling water and facilitated the transport of the oil-loaded sorbent near the sea.

Reusability and Recoverability of the Sorbed Oil

Recent interest in the development of oil sorbents has focused on the production of porous structured fibers to enhance their SSA and porosities to further promote the oil-sorption capacity.[31] Nevertheless, one fatal issue porous structured fibrous sorbents encounter is that these structures may compromise their mechanical properties, including their fiber strength and elasticity, and this weakens their reusability accordingly.[21]

Figure 9 shows the oil-sorption/desorption operation process. The sorption capacities of D4 and S4 for motor oil at different sorption/desorption cycle are illustrated in Figure 10. We observed that the sorption capacity of D4 decreased slightly throughout the whole process, whereas the sorption capacity of S4 decreased sharply by about 17% in the second cycle, and a slight and continuous decrease in the sorption capacity was observed after the third cycle. For these two fibers, the sorption values both remained at around 80 g/g throughout the subsequent cycles. After seven sorption/desorption cycles, the decrease in the sorption capacity did not exceed 23%, and a sorption capacity of 81 g/g was still maintained; this was approximately three to four times that of the commercial PP nonwoven. At the same time, a large margin of above 97% oil could be recovered from the oil-loaded sorbent; this indicated an excellent recoverability of adsorbed oil. The inherent molecular structure, smooth surface, and solid interior morphology of the as-spun fibers contributed to its superior mechanical properties and thus reusability. The decrease in the oil-sorption capacity was mainly attributed to the irreversible deformation and collapse of interfiber voids after the mechanical squeezing caused by the vacuum pump.

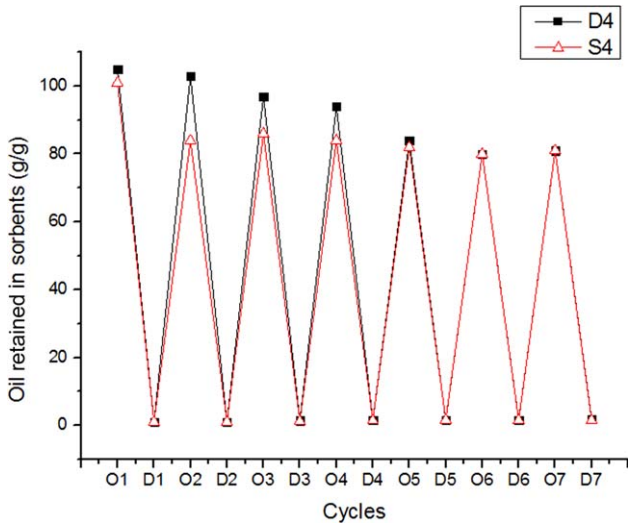

Figure 10. Oil retained in S4 and D4 versus the sorption/desorption cycles. O1–O7 indicate the oil-sorption conditions, and D1–D7 indicate the oil desorption conditions. [Color figure can be viewed in the online issue, which is available at wileyonlinelibrary.com.]

CONCLUSIONS

The controllable preparation of an oil sorbent based on MES is discussed in this article. Ultrafine PP fibers ranging from 1.89 to 7.32 μm with different porosities were fabricated with a self-designed MES device by the manipulation of the electric field. The maximum oil-sorption capacities of the resulting fibers for oil motor oil and peanut oil were 129 and 80 g/g, respectively; these values were six to seven times higher than that of the commercial PP nonwoven for the corresponding oils. The high oil-sorption capacity of the melt-electrospun PP fibers was attributed to its small fiber diameter, high porosity, olephilicity, and hydrophobicity. We found that the porosity played a paramount role in determining the sorption capacity of the fibers in the microscale. Additionally, the superior mechanical performance of the resulting fibers ensured their reusability and recoverability. They could be reused at least seven times while still maintaining a sorption capacity of around 80 g/g, and above 97% of the sorbed oil could be recovered. In contrast to SES, MES is simpler, more cost effective, and environmentally friendly because of the elimination of the solvent. Furthermore, through the application of a needleless nozzle, the goal of the industrial-scale production of the PP oil sorbent is achievable. In conclusion, we do believe that solvent-free MES holds great promise for the fabrication of microfibers or even nanofibers in marine oil-spill cleanup and other oil–water separation applications.

REFERENCES

1. Sidik, S. M.; Jalilb, A. A.; Triwahyono, S.; Adam, S. H.; Satar, M. A. H.; Hameed, B. H. *Chem. Eng. J.* **2012**, *203*, 9.

2. Wang, J. T.; Zheng, Y. A.; Wang, A. Q. *Ind. Crops Prod.* **2012**, *40*, 178.
3. Wang, J.; Zheng, Y.; Wang, A. *Chem. Eng. J.* **2012**, *213*, 1.
4. Adebajo, M. O.; Frost, R. L.; Kloprogge, J. T.; Carmody, O.; Kokot, S. *J. Porous Mater.* **2003**, *10*, 159.
5. Sayed, S. A.; Zayed, A. M. *Desalination* **2006**, *194*, 90.
6. Zhu, Q.; Pan, Q.; Liu, F. *J. Phys. Chem.* **2011**, *115*, 17464.
7. Yu, Q.; Tao, Y.; Huang, Y.; Lin, Z.; Zhuang, Y.; Ge, L.; Shen, Y.; Hong, M.; Xie, A. *Ind. Eng. Chem. Res.* **2012**, *51*, 8117.
8. Deschamps, G.; Caruel, H.; Borredon, M. E.; Bonnie, C.; Vignoles, C. *Environ. Sci. Technol.* **2003**, *37*, 1013.
9. Guix, M.; Orozco, J.; Garcia, M.; Gao, W.; Sattayasamitsathit, S.; Merkoci, A.; Escarpa, A.; Wang, J. *ACS Nano* **2012**, *6*, 4445.
10. Maja, M. R.; Dragan, M. J.; Petar, M. J.; Zoran, L. J. P.; Helga, F. T. *Environ. Sci. Technol.* **2003**, *37*, 1008.
11. Jose, A. Q.; Gaurav, P.; Robert, P. *Ind. Eng. Chem. Res.* **2009**, *48*, 191.
12. Li, D.; Zhu, F.; Li, J.; Na, P.; Wang, N. *Ind. Eng. Chem. Res.* **2013**, *52*, 516.
13. Bhardwaj, N.; Kundu, S. C. *Biotechnol. Adv.* **2010**, *28*, 325.
14. Hutmacher, D. W.; Dalton, P. D. *Chem. Asian J.* **2011**, *6*, 44.
15. Lyons, J.; Li, C.; Ko, F. *Polymer* **2004**, *45*, 7597.
16. Zhu, H.; Qiu, S.; Jiang, W.; Wu, D.; Zhang, C. *Environ. Sci. Technol.* **2011**, *45*, 4527.
17. Wu, J.; Wang, N.; Wang, L.; Dong, H.; Zhao, Y.; Jiang, L. *Appl. Mater. Interfaces* **2012**, *4*, 3207.
18. Lin, J.; Shang, Y.; Ding, B.; Yang, J.; Yu, J.; Al-Deyab, S. S. *Mar. Pollut. Bull.* **2012**, *64*, 347.
19. Lin, J.; Ding, B.; Yang, J.; Yu, J.; Sun, G. *Nanoscale* **2012**, *40*, 176.
20. Lin, J.; Tian, F.; Shang, Y.; Wang, F.; Ding, B.; Yu, J. *Nanoscale* **2012**, *4*, 5316.
21. Lin, J.; Tian, F.; Shang, Y.; Wang, F.; Ding, B.; Yu, J.; Guo, Z. *Nanoscale* **2013**, *5*, 2745.
22. Dalton, P. D.; Grafahrend, D.; Klinkhammer, K.; Klee, D.; Möller, M. *Polymer* **2007**, *48*, 6823.
23. Liu, Y.; Deng, R.; Hao, M.; Yan, H.; Yang, W. *Polym. Eng. Sci.* **2010**, *50*, 2074.
24. McHale, G. *Langmuir* **2007**, *23*, 8200.
25. Miline, A. J.; Amirfazli, A. *Adv. Colloid Interface Sci.* **2012**, *170*, 48.
26. Cho, D.; Zhou, H.; Cho, Y.; Audus, D.; Joo, Y. L. *Polymer* **2010**, *51*, 6005.
27. Wang, J.; Zheng, Y.; Wan, A. *Mar. Pollut. Bull.* **2013**, *69*, 91.
28. Arbatan, T.; Fang, X.; Shen, W. *Chem. Eng. J.* **2011**, *166*, 787.
29. Wei, Q. F.; Mather, R. R.; Fotheringham, A. F.; Yang, R. D. *Mar. Pollut. Bull.* **2003**, *46*, 780.
30. Rengasamy, R. S.; Das, D.; Karan, C. P. *J. Hazard. Mater.* **2011**, *186*, 526.
31. Lin, J.; Ding, B.; Yu, J.; Hsieh, Y. *ACS Appl. Mater. Interfaces* **2010**, *2*, 521.